Proceedings of the XVIII ECSMGE 2024
GEOTECHNICAL ENGINEERING CHALLENGES
TO MEET CURRENT AND EMERGING NEEDS OF SOCIETY

ISBN 978-1-032-54816-6
DOI 10.1201/9781003431749-46

Application of optimization algorithms in geotechnical engineering as decision-making support tool

Application des algorithmes d'optimisation en génie géotechnique comme outil de soutien à la prise de décision

K. Cerek*, E. Hadjiloo, J. Grabe
Hamburg University of Technology, Hamburg, Germany
*kacper.cerek@tuhh.de

ABSTRACT: This paper advocates for climate-responsive optimization in civil engineering, leveraging the NSGA-II algorithm. Conducting an in-depth study on a dike structure, the integration of pymoo with Plaxis 2023.2 via Python emerges as a potent decision support tool. Employing a plane strain approach with 15-noded triangular elements, the numerical model undergoes SRFEA for stability assessment. Three objectives, material demand (f1), LC2 exploitation (f2), and LC3 exploitation (f3), are systematically minimized by NSGA-II. Results, depicted in a Pareto surface, spotlight a wider spread for material demand, emphasizing its variability. Findings underscore the pivotal role of multi-objective algorithms in guiding sustainable civil engineering decisions amid climate change challenges.

RÉSUMÉ: Cet article plaide en faveur de l'optimisation adaptative au climat dans le génie civil, en exploitant l'algorithme NSGA-II. En menant une étude approfondie sur une structure de digue, l'intégration de pymoo avec Plaxis 2023.2 via Python émerge comme un puissant outil de soutien à la décision. En utilisant une approche de contrainte simple avec des éléments triangulaires à 15 nœuds, le modèle numérique fait l'objet d'une analyse de stabilité par SRFEA. Trois objectifs, la demande de matériaux (f1), l'exploitation LC2 (f2) et l'exploitation LC3 (f3), sont systématiquement minimisés par NSGA-II. Les résultats, représentés dans une surface de Pareto, mettent en lumière une plus grande variabilité de la demande de matériaux. Les conclusions soulignent le rôle central des algorithmes multi-objectifs dans la conduite de décisions durables en génie civil face aux défis du changement climatique.

Keywords: SRFEA; Multi-objective evolutionary algorithm; NSGA-II; decision support tool; dikes.

1 INTRODUCTION

The impact of climate change is compelling the civil engineering sector to prioritize the optimization of constructed structures. Geotechnical engineering frequently encounters the challenge of designing structures that must satisfy diverse objectives. The decision-making process regarding which solution to adopt for the final design is often intricate and far from straightforward.

This study is dedicated to present the advantages of employing a multi-objective evolutionary algorithm, NSGA-II, for the purpose of identifying trade-offs among various objectives. To achieve this, an extensive investigation of a dike structure has been undertaken in this paper, with the aim of discovering the most optimal solutions for three distinct objective functions.

2 GENERAL INFORMATION

2.1 Decision-making support tool

The following study presents implementation of a decision-making support tool, which enables users to make more reasonable and more optimal decisions considering their geotechnical problem. The presented routine incorporates multi-objective optimization framework *pymoo* (Blank and Deb, 2020) and integrates it via Python programming language (Van Rossum and Drake, 2009) with FEM-software Plaxis 2023.2 (Plaxis, 2023).

This paper implements the multi-objective Nondominated Sorting Genetic Algorithm (NSGA-II) from Deb et al. (2002), which offers an elitist-preserving approach. The NSGA-II combines a random parent population with its offspring in order to find a set of trade-offs which are represented by a Pereto-front, or a Pareto-surface, if there are more than two objectives defined. The algorithm has been succefully applied for solving multi-objective geotechnical problems, e.g. Cerek and Grabe (2023), Cerek et al. (2023) and Das et al. (2016).

The self-programmed Python code triggers the FEM-simulations which deliver searched results. The outcomes are then evaluated by NSGA-II algorithm and the process repeats itself until predefined termination criteria are met. More to selection process of optimal solutions and set up of the algorithm can be found in Cerek and Grabe (2023) and Cerek et al. (2023). Once a set of trade-offs are found, the algorithm stops and a pareto-surface is displayed, where a user may find the problem‘s optimal solutions for defined objectives. Based on that, a fully aware decision might be made taken all important objectives into account.

Table 1. Soil parameters applied in FEM-model.

	Unit	Clay 1	Clay 2	Sand 1	Sand 2
γ_{unsat} (unsaturated unit weight)	(kN/m³)	16.0	15.0	18.0	19.0
γ_{sat} (saturated unit weight)	(kN/m³)	16.0	15.0	20.0	21.0
E' (Young´s modulus)	(MN/m²)	2.5	2.0	20.0	40.0
ν' (Poisson‘s ratio)	(-)	0.3	0.3	0.2	0.2
c' (effective cohesion)	(kN/m²)	10.0	10.0	0.1	0.1
s_u (undrained shear strength)	(kN/m²)	25.0	20.0	-	-
φ'* (effective friction angle)	(°)	17.5	17.5	30.0	35.0
ψ' (dilatancy angle)	(°)	0.0	0.0	5.0	5.0
$k_{x/y}$ (horizontal/vertical permeability)	(m/s)	1.0E^{-9}	1.0E^{-10}	1.0E^{-4}	1.0E^{-4}

* For undrained conditions, effective friction angle φ' = 0.0°

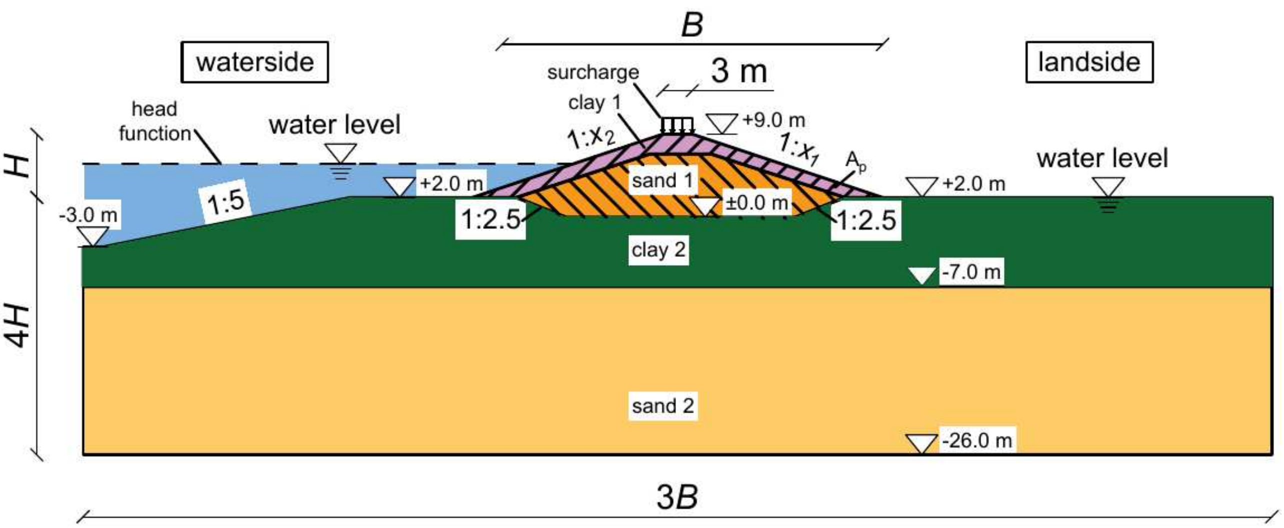

Figure 1. Model geometry.

2.2 Strength reduction finite element analysis (SRFEA)

In this research, all numerical simulations were performed using the commercial displacement-based finite element software Plaxis 2023.1 (Plaxis, 2023). The SRFEA was employed, which provides a Factor of Safety (FoS). The soil strength parameters were reduced until structural collapse was observed. Equation 1 outlines the formulation of FoS, with c', φ', and s_u representing the effective cohesion, effective friction angle, and undrained shear strength, respectively. The safety factors were not incorporated in our simulations, and all values represent characteristic data. Additionally, it's worth noting that, in the case of undrained shear strength, we solely applied a straightforward reduction of s_u.

$$FoS = \frac{\tan \varphi'}{\tan \varphi'_{mob}} = \frac{c'}{c'_{mob}} = \frac{s_u}{s_{u,mob}} \quad (1)$$

3 NUMERICS

3.1 Numerical model

The finite element model employs a plane strain approach, employing 15-noded triangular elements. To ensure a dependable Factor of Safety (FoS), we meticulously refined the mesh by opting for a relative element size of 0.015. The total count of finite elements fluctuates based on individual model setups. In the interest of computational efficiency, we employed a coarser mesh for the lower soil layer without compromising model accuracy. Conversely, the mesh along the dike crest underwent refinement to accommodate the application of a line load.

In the scope of this study, we adopted a Mohr-Coulomb failure criterion. The model encompassed four distinct soil layers. It should be pointed out that fine-grained soil layers are modelled for undrained conditions, since quick loading rate is occuring within the simulation. The soil properties, as detailed in Table 1, and the model geometry, including the soil layers, are visually represented in Figure 1.

3.2 Model geometry

The selection of dimensions for the numerical model was guided by the recommendations provided by Mestat et al. (2004). These recommendations are based on correlations between the height of the dike *H* and the overall model depth, as well as between the width of the dike *B* and the total model width. The geometric configuration of the system is further characterized by two parametric variables, denoted as x_1 and x_2, which represent the horizontal components of the slope.

3.3 Calculation phases and loads

The model comprises four consecutive calculation phases. The initial phase, referred to as LC0, utilizes gravity loading to establish initial stresses. Subsequently, a plastic Nil-step phase (LC1) is executed, followed by a fully coupled flow-deformation analysis phase (LC2). In LC2, a head function is applied to the water level on the waterside of the dike. In the subsequent plastic calculation phase (LC3), a uniformly distributed surcharge load of 10.0 kN/m² is applied to the dike crest. Both LC2 and LC3 are followed by a safety analysis that incorporates SRFEA, as described in Section 2.2 of this paper.

Throughout all phases, the water level on the landside remains constant. In contrast, on the opposite side, it is initially set at +2.0 m. During the transient calculation phase, the water level progressively rises in a linear fashion up to +5.0 m. The critical load cases are indicated in Figure 1.

4 OPTIMIZATION PROBLEM

4.1 Problem definition

4.1.1 Variables

The geometry of the numerical model is parametrised by the horizontal components of the slope, as mentioned in Section 3.2. The lower boundaries x_l and upper boundaries x_u are given by Equations 2-3. The rounding of variables during the optimization process was set to two decimal places.

$$x_l = \{1.5; 1.5\} = \{x_{1,min}; x_{2,min}\} \quad (2)$$

$$x_u = \{4.5; 4.5\} = \{x_{1,max}; x_{2,max}\} \quad (3)$$

4.1.2 Objectives

This study delves into the intricacies of an optimization problem characterized by three semi-independent objectives, each represented by specific objective functions: f_1, f_2, and f_3 as detailed in Equations 4-6. Over successive algorithm generations, all objective functions are systematically minimized. Function f_1 pertains to the material demand A_p that is expresses by cross-sectional area. Both functions f_2 and f_3 are formulated as reciprocals of their respective *FoS* obtained from calculation phase LC2 or LC3.

$$f_1 = A_p \quad (4)$$

$$f_2 = \frac{1}{FoS_{LC2}} \quad (5)$$

$$f_3 = \frac{1}{FoS_{LC3}} \quad (6)$$

Consequently, optimization is performed for both horizontal components of the slope on the landside and waterside. This optimization is carried out with regard to minimizing material demand and ensuring a satisfactory factor of safety, both during the coupled flow-deformation analysis phase (LC2) and the plastic calculation phase (LC3).

5 STUDIES

This paper focuses on the multi-objective optimization of a dike structure using the NSGA-II algorithm. The algorithm, with an initial population of 100, was employed for this purpose. The termination criterion for design space tolerance was set to two decimal places, checked every second iteration to ensure a diverse range of outcomes.

Figure 2 depicts the results obtained from the optimization process. It is evident that the spread of solutions for the objective f_1 (material demand) is notably wider compared to f_2 and f_3. The Pareto surface aids the decision-making process for the final design by offering an overview of possibilities.

The variables resulting from the optimization process are illustrated in Figure 3. It can be concluded that, for the selected objectives corresponding to defined load cases, a design with a steeper slope on the waterside is preferable, as the spread of solutions for this side is smaller. Conversely, results for the landside slope vary between the lower and upper boundaries.

Table 2 provides exemplary results for variables and objectives resulting from the optimization process (Sol1, Sol2), as well as for a traditional design (Sol3). It is crucial to emphasize that the difference in material demand between the presented solutions Sol1 and Sol2 is nearly 90%. This implies that choosing a design with a smoother landside slope would lead to a substantial increase in costs, CO_2 footprint, and construction time. It should also be mentioned that the traditional design Sol3 would collapse under the applied surcharge load in LC3, even though it has flatter slopes and requires about 85% more material than Sol1.

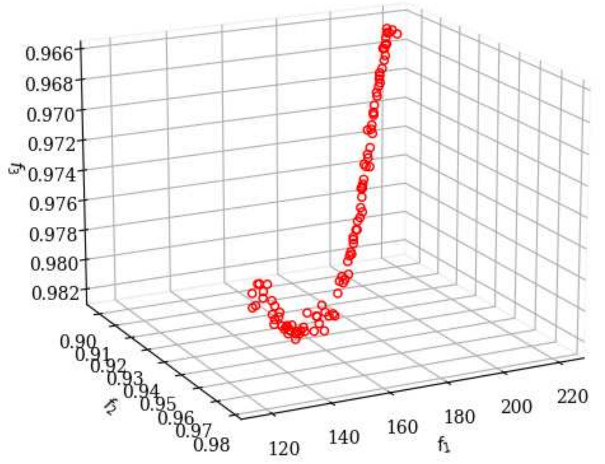

Figure 2. Pareto surface illustrating the optimization of three-objectives problem: f_1 – material demand; f_2 – exploitation for LC2; f_3 – exploitation for LC3.

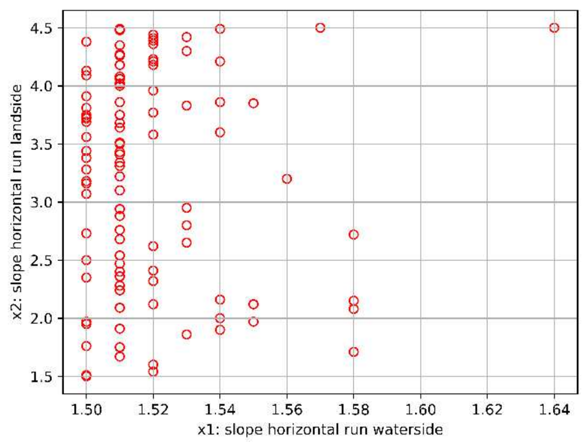

Figure 3. Results illustrating the optimization process variables x_1 and x_2 (horizontal components of the slope).

Table 2. Exemplary results of optimization process

	x_1	x_2	f_1	f_2	f_3
Sol1	1.50	1.51	117.65	0.98	0.98
Sol2	1.64	4.50	221.47	0.90	0.97
Sol3	3.00	3.00	216.60	0.95	>1.00

6 CONCLUSIONS

The study presented in this paper demonstrates that the application of multi-objective algorithms in the design process enhances problem understanding and provides a diverse set of solutions, which can be evaluated based on predefined objectives. The proposed routine, incorporating Finite Element Method (FEM) simulation and optimization techniques, has proven to be a valuable decision support tool in the design process, especially when dealing with numerous objectives that are challenging for classical human evaluation.

The adoption of this approach empowers engineers to make informed decisions, contributing to the creation of more sustainable structures. Consequently, it aids in the reduction and deceleration of climate changes caused by the civil engineering industry.

REFERENCES

Blank, J., Deb, K. (2020): Pymoo: Multi-Objective Optimization in Python. In IEEE Access 8, pp. 89497–89509. DOI: 10.1109/ACCESS.2020.2990567.

Cerek, K., Grabe, J. (2023): Numerical simulation and optimization of dike geometry using multi-objective evolutionary algorithm NSGA-II. In ISSMGE. DOI: 10.53243/NUMGE2023-80.

Cerek, K., Hadjiloo, E., Grabe, J. (2023): Sustainable dike adaptation measures using finite element method and optimization algorithm NSGA-II. (manuscript accepted). In GEOTEC Hanoi 2023.

Das, M.R., Purohit, S., Das, S.K. (2016): Multi-objective Optimization of Reinforced Cement Concrete Retaining Wall. In Indian Geotech J 46 (4), pp. 354–368. DOI: 10.1007/s40098-015-0178-y.

Deb, K., Pratap, A., Agarwal, S., Meyarivan, T. (2002): A fast and elitist multiobjective genetic algorithm: NSGA-II. In IEEE Trans. Evol. Computat. 6 (2), pp. 182–197. DOI: 10.1109/4235.996017.

Mestat, Ph., Bourgeois, E., Riou, Y. (2004): Numerical modelling of embankments and underground works. In Computers and Geotechnics 31 (3), pp. 227–236. DOI: 10.1016/j.compgeo.2004.01.003.

PLAXIS (2023): PLAXIS 2D 2023.1 Reference Manual. Edited by Bentley.

Van Rossum, G., Drake, F. L. (2009): Python 3 Reference Manual.: CA: CreateSpace.